Aeroacoustics Conferences
26-29 May 2026, Brussels, Belgium
32nd AIAA/CEAS Aeroacoustics Conference (2026)
10.2514/6.2026-3217

Numerical Investigation of Mode Scattering in Bifurcated Annular Ducts

Hugo Vincent *, Antonio Pereira †, and Marc C. Jacob ‡
Ecole Centrale de Lyon, CNRS, Univ Claude Bernard Lyon 1, INSA Lyon, LMFA, UMR5509, 69130, Ecully, France

Maximilian Behn § and Ulf Tapken ¶
German Aerospace Center (DLR), Institute of Propulsion Technology, Berlin, Germany

The scattering of sound waves by pylons (struts) in annular ducts is investigated numerically in quiescent conditions and with mean flows at Mach numbers ranging from 0.1 to 0.4. To this end, the propagation of acoustic modes in configurations with two or three pylons is computed over a wide frequency range using a frequency-domain finite-element solver. The transmitted and reflected duct modes are estimated using the single-plane pressure/velocity matching method. The sound pressure levels and modal amplitudes obtained are compared with experimental data, showing good overall agreement and thereby supporting the validity of the numerical approach. The amplitudes of the reflected and transmitted modes are found to depend strongly on the number of pylons and on frequency. The number of pylons governs the set of scattered azimuthal modes in agreement with the Tyler-Sofrin rule. At high frequencies, the scattering becomes broader as additional azimuthal and radial modes become cut on. For incident plane waves, the strongest reflected components are associated with azimuthal orders close to cut-off. For incident spinning modes, the scattered field is shown to follow the same selection rule, while the dominant transmitted component may, in some cases, have an azimuthal order of opposite sign to that of the incident mode, indicating a reversal of the spinning direction through the pylon row. The influence of mean flow on the scattered levels is significant but non-monotonic, with variations that depend on frequency, mode order, and number of pylons.

I. Introduction

Aircraft noise exposure continues to pose health risks to populations residing near airports. The introduction of Ultra-High Bypass Ratio (UHBR) engines has reduced the predominance of jet noise, making fan-stage noise the principal contributor to overall aircraft noise, as discussed in the recent review by Moreau [1]. The fan-noise spectrum contains strong tonal components at the blade passing frequency and its harmonics [2–4]. Moreover, the associated acoustic field exhibits well-defined spinning modes governed by the rotor and stator blade count [5]. The noise propagates both downstream and upstream of the fan stage. Downstream, it travels through the bypass duct and is scattered by bifurcations, such as pylons or struts, before radiating to the far field [6–8].

Several authors have shown that the presence of bifurcations leads to strong scattering of the noise into a wide range of azimuthal modes [9–12]. Among the various parameters affecting sound scattering, the pylon geometry has been identified as a key governing factor in numerous studies [13–16]. In particular, Panek et al. [16] reported that the amplitudes of reflected modes are stronger for thicker pylons. In contrast, the effects of the number of pylons and mean flow have received relatively little attention. Nonetheless, the numerical study by Schonwald et al. [17] specifically investigated the effects of mean flow, showing that introducing a mean flow at Mach 0.43 leads to a stronger azimuthal and radial scattering, and amplifies certain modes, particularly at higher radial orders.

Given the above, Behn et al. [18] very recently performed experiments to examine the influence of the number of pylons in detail, exciting dominant acoustic modes over a wide frequency and mode order range using a loudspeaker array in annular ducts containing two or three pylons [19, 20]. In parallel, Girier & Leclère [21] address the same configuration from an analytical perspective, employing a mode-matching formulation combined with a slowly-varying duct approach.

*Post-doctoral fellow, Ecole Centrale de Lyon, Laboratoire de Mécanique des Fluides et d'Acoustique, France, hugo.vincent@ec-lyon.fr
†Research Engineer, Ecole Centrale de Lyon, Laboratoire de Mécanique des Fluides et d'Acoustique, France, antonio.pereira@ec-lyon.fr
‡Professor, Ecole Centrale de Lyon, Laboratoire de Mécanique des Fluides et d'Acoustique, France, Member AIAA, marc.jacob@ec-lyon.fr
§Research Engineer, Engine Acoustics Department, Bismarckstraße 101, 10625 Berlin, Germany, Member AIAA, maximilian.behn@dlr.de
¶Research Scientist, Engine Acoustics Department, Bismarckstraße 101, 10625 Berlin, Germany, ulf.tapken@dlr.de

In the present work, numerical simulations are performed for the same geometries. A first objective is to validate the numerical approach against the experimental data of Behn et al. [18]. A second objective is to analyze in greater depth how the number of pylons and the presence of mean flow affect the reflection and transmission of acoustic modes. To this end, the propagation of a large set of incident modes is computed at several frequencies using the commercial frequency-domain finite-element solver Actran™. The reflected and transmitted modal contents are then estimated using the single-plane pressure/velocity matching method [22].

The paper is organized as follows. First, the geometries, flow configurations, and numerical methods are described. The propagation of incident plane waves in the ducts with two and three pylons is then examined in quiescent conditions. The azimuthal modal content obtained numerically is subsequently compared with the experimental measurements in order to assess the validity of the simulations. The reflected and transmitted modal spectra are then analyzed as functions of frequency and pylon number. Results obtained for incident higher-order azimuthal modes are thereafter discussed. Finally, the influence of a non-uniform mean flow on the acoustic scattering is investigated.

II. Methods and parameters

A. Simulation parameters

The annular ducts with two or three pylons under consideration are shown in Figures 1(a,b). The inner and outer radii are 0.165 m and 0.25 m, respectively, and the pylon length is 0.75 m. These dimensions match those used in the experiments by Behn et al. [18]. In the simulations, however, the ducts are extended to six pylon lengths in order to analyze the acoustic scattering in greater detail. In the experiments, quasi-anechoic terminations are used, and a prescribed duct mode is generated using two circumferential rings of 16 loudspeakers. The reader is referred to Behn et al. [18] for a detailed description of the experimental setup.

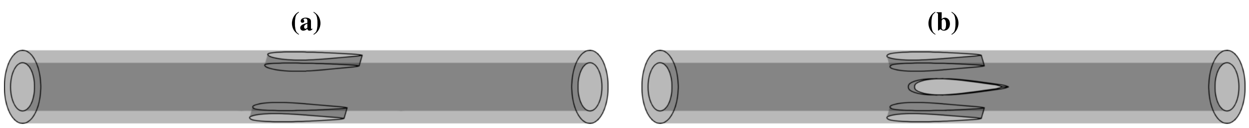

Fig. 1 Representations of the annular ducts with (a) two pylons and (b) three pylons.

Four frequencies, namely 400, 800, 1600, and 3200 Hz, are considered, together with five flow configurations including the no-flow case. In quiescent conditions, the acoustic wavelength is comparable to the pylon length at $f = 400$ Hz and decreases to about one-eighth of the pylon length at $f = 3200$ Hz. The cut-on frequencies of the annular duct modes in the absence of flow are shown in Figure 2, together with the frequencies investigated in the simulations. For the three lowest frequencies, only modes of radial order $n = 0$ are cut on, whereas modes with $n = 1$ also become cut on at $f = 3200$ Hz. Regarding the azimuthal order m, only modes such that $|m| < 1$ are cut on at $f = 400$ Hz. This limit increases to $|m| < 3$, $|m| < 6$, and $|m| < 12$ at $f = 800$, 1600, and 3200 Hz, respectively.

The mean-flow cases correspond to axial Mach numbers of 0.1, 0.2, 0.3, and 0.4. They are computed with Actran™ assuming a potential flow. The resulting velocity magnitude fields for the two ducts are shown in Figure 3, where flow goes from left to right. As expected from mass conservation, peak velocities are observed in the pylon section, whereas lower values occur in the vicinity of the pylon leading edges.

B. Numerical methods

The propagation of duct acoustic modes is computed using the commercial finite-element code Actran™, which solves a frequency-domain formulation of Möhring's equation [23]. At the upstream and downstream boundaries, modal boundary conditions prescribe a single incident duct mode and avoid reflections. The two ducts are discretized with fine unstructured meshes of about 1.2 million second-order tetrahedra generated using the open-source software Gmsh [24]. The element size is nearly uniform over the computational domains and was selected based on a mesh-convergence study. A minimum of four quadratic elements per shortest acoustic wavelength was ensured, with the wavelength estimated as $\lambda_{\min} = (c - U)/f$, where c is the ambient sound speed and U is the axial mean-flow velocity. The simulations are not expensive in terms of numerical cost. In this paper, the solutions of 104 simulations are analyzed by varying the frequency, the number of pylons, and the incident azimuthal mode. They constitute a database of around 60 GB.

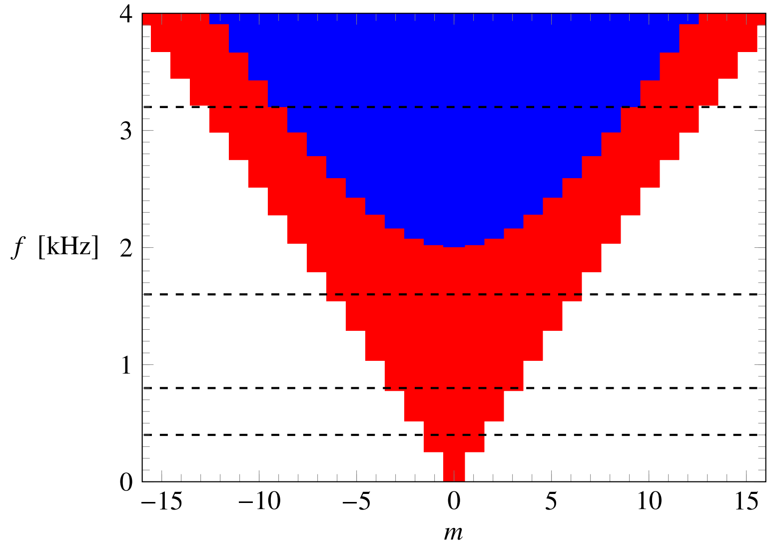

Fig. 2 Cut-on frequencies of the azimuthal modes with radial orders $n = 0$ and $n = 1$; - - - - - frequencies considered for the simulations.

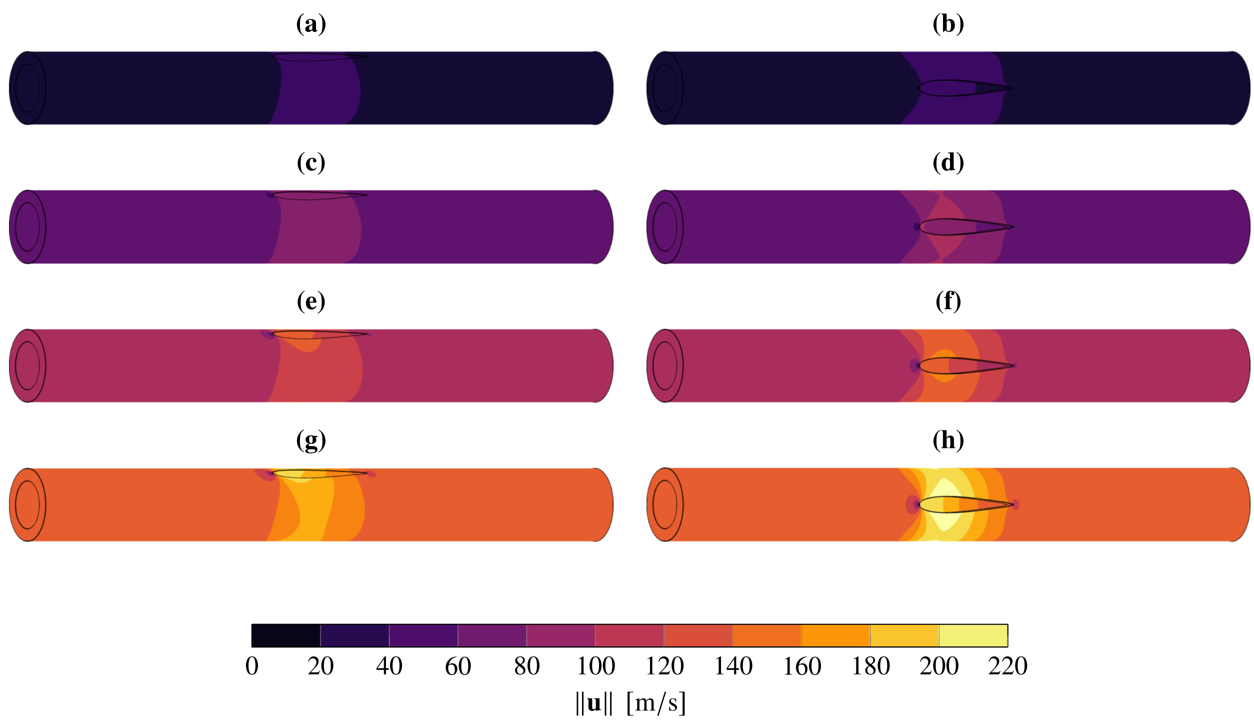

Fig. 3 Representations of the velocity magnitude fields for the duct with (first column) two pylons and (second column) three pylons, for (first row) M = 0.1, (second row) M = 0.2, (third row) M = 0.3, and (fourth row) M = 0.4.

To assess the validity of the simulations, the circumferential ring of 33 regularly spaced microphones located upstream of the pylons in the experiments by Behn et al. [18] is included in the computational setup. The simulated pressure field values are interpolated onto the sensor positions via an inverse-distance-weighted linear interpolation. The complex Fourier coefficients of the pressure at each sensor are post-processed using identical procedures for the experiment and the simulation.

In addition, duct mode decompositions are carried out with Actran™ to estimate the sound power levels of both reflected and transmitted modes. It is assumed that the pressure fields can be decomposed as

$$p\left(r,\theta,z\right)=\sum_{m=-\infty}^{\infty}\sum_{n=0}^{\infty}\left(A_{m,n}e^{ik^{+}_{z_{m,n}}z}+B_{m,n}e^{ik^{-}_{z_{m,n}}z}\right)f_{m,n}\left(r\right)e^{im\theta}\,, \tag{1}$$

where $A_{m,n}$ and $B_{m,n}$ are the amplitudes of the downstream- and upstream-propagating modes associated with the annular-section eigenfunctions $f_{m,n}$. $k^{+}_{z_{m,n}}$ and $k^{-}_{z_{m,n}}$ are the associated axial wavenumbers, and i is the imaginary unit. The decomposition is performed with the single-plane pressure/velocity matching method of Rienstra [22]. It is carried out at the upstream microphone ring and at a downstream section symmetric with respect to the pylons. This allows us to estimate the amplitudes of the reflected and transmitted propagating azimuthal and radial modes.

III. Results

A. Plane wave propagation without flow

To first illustrate the propagation of plane acoustic waves in the ducts with two and three pylons, the pressure fields obtained without flow at $f = 400$, 800, 1600, and 3200 Hz are shown on the outer duct surface in Figures 4(a-d) for the two-pylon configuration and in Figures 4(e-h) for the three-pylon configuration. At $f = 400$ Hz, shown in Figures 4(a,e), the acoustic wavelength is comparable to the pylon length. At this frequency, for both geometries, the plane wave propagates through the pylon row with no visible reflection. By contrast, for $f \geq 800$ Hz, the propagation is clearly altered by the pylons, and azimuthal patterns become visible upstream and downstream of the pylon section. This indicates that the pylon row scatters the incident plane wave into non-axisymmetric azimuthal modes. In particular, at $f = 1600$ Hz in Figures 4(c,g), six maxima can be identified around the annulus upstream of the pylons, suggesting a strong contribution of modes with azimuthal order $m = \pm 6$. More generally, the azimuthal order of the dominant reflected pattern increases with frequency. For the three-pylon duct, for instance, the dominant reflected structure appears to correspond approximately to $m = \pm 3$ at 800 Hz, $m = \pm 6$ at 1600 Hz, and $m = \pm 12$ at 3200 Hz. This trend is consistent with the fact that additional azimuthal orders become cut on as the frequency increases. These observations suggest that the scattering process redistributes the incident energy over a limited number of azimuthal modes imposed by the pylon geometry. This qualitative behavior is analyzed more quantitatively in the following through modal decompositions and sound-power-level comparisons.

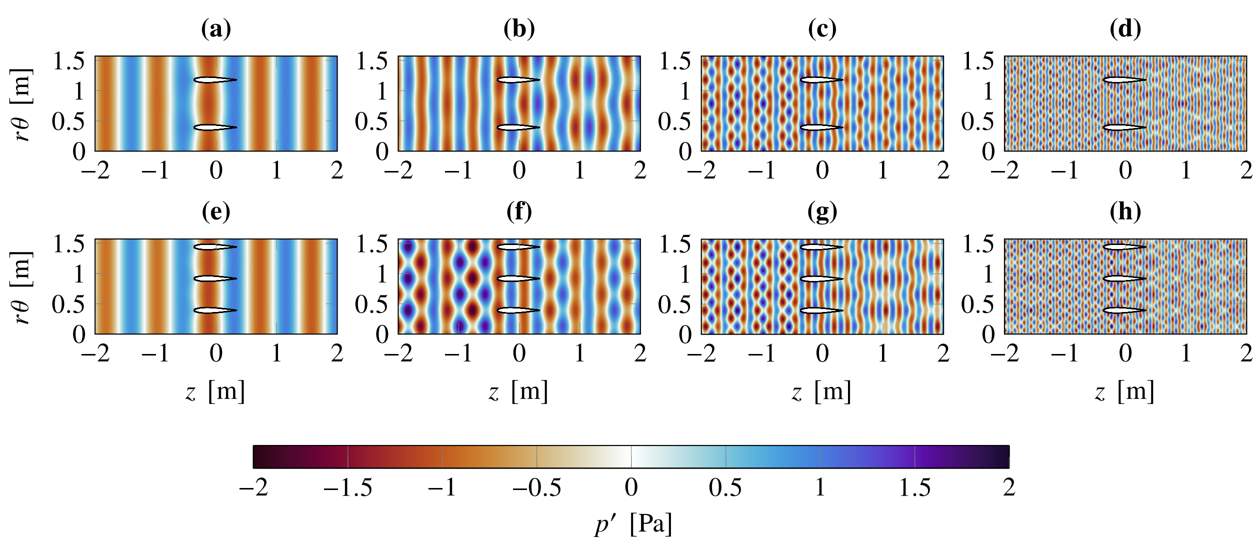

Fig. 4 Pressure fields obtained for incident plane wave for the annular ducts with (first row) two pylons and (second row) three pylons for (a,e) $f = 400$ Hz, (b,f) $f = 800$ Hz, (c,g) $f = 1600$ Hz, and (d,h) $f = 3200$ Hz.

B. Comparison with experiments

To assess the validity of the numerical simulations, the contributions of the azimuthal modes to the SPL measured upstream of the pylons are plotted for the four frequencies and the two configurations in Figures 5(a-d) and 5(e-h). The corresponding experimental results and the cut-off limit of the first non-propagating azimuthal modes are also shown. For each case, the SPLs are normalized by their maximum value, which is obtained for the axisymmetric mode, as expected for an incident plane wave. Overall, the numerical and experimental modal spectra are in good agreement for all cases, which supports the validity of the simulations.

Because the incident field is axisymmetric and the pylons are uniformly distributed in azimuth, the spectra obtained using the simulations are symmetric with respect to $m = 0$, that is, the levels at $+|m|$ and $-|m|$ are identical. This symmetry is not always observed in the experimental results, especially at 3200 Hz in Figures 5(d,h), which may be attributed to residual reflections at the quasi-anechoic terminations and to imperfections in the loudspeaker-array excitation. At the lowest frequency, shown in Figures 5(a,e), significant levels are obtained only for the axisymmetric mode because the azimuthal orders expected from scattering are cut off. For $f \geq 800$ Hz, contributions appear at azimuthal orders consistent with the geometric periodicity of the pylon row. For the two-pylon duct, only orders of the form $m = \pm 2k$ are observed in Figures 5(b-d), whereas for the three-pylon duct the scattered content is restricted to orders $m = \pm 3k$ in Figures 5(f-h), with $k \in \mathbb{N}$ and only cut-on modes contributing. This modal selection is consistent with the Tyler-Sofrin rule [5], here applied to a purely geometric periodicity imposed by the pylon row. The strongest modal contributions are generally associated with azimuthal orders close to cut-off, in agreement with the numerical observations reported by Panek et al. [16]. For instance, at $f = 1600$ Hz the largest levels are obtained for $m = \pm 6$, which correspond to the highest cut-on azimuthal orders at that frequency. This is also consistent with the spatial patterns observed upstream of the pylons in Figure 4.

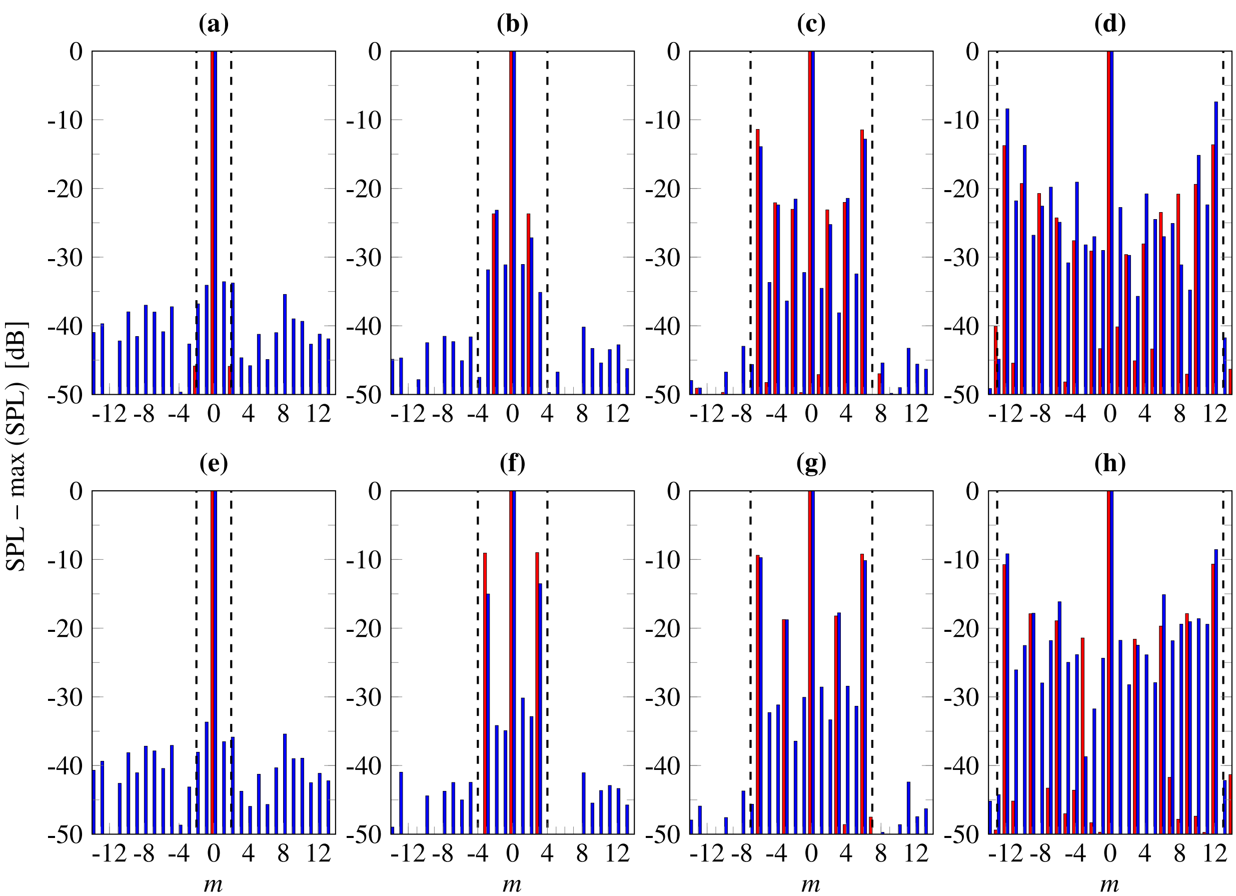

Fig. 5 Contributions of the azimuthal modes in a section upstream of the pylons for the duct with (first row) two pylons and (second row) three pylons, obtained with ▬ numerical simulations and ▬ experiments for (a,e) f = 400 Hz, (b,f) f = 800 Hz, (c,g) f = 1600 Hz, and (d,h) f = 3200 Hz; - - - - - first cut-off azimuthal mode.

C. Analysis of the reflected and transmitted modes

The sound power levels associated with the reflected and transmitted azimuthal modes are plotted for all frequencies and both geometries in Figures 6 and 7. The reflected contributions are obtained from the amplitudes of the upstream-propagating modes evaluated upstream of the pylon row, whereas the transmitted contributions are obtained downstream of the pylons using the modal decomposition described above.

For the reflected field, all cut-on azimuthal modes compatible with the geometric periodicity are excited. In the two-pylon configuration, the reflected content is therefore restricted to orders $m = \pm 2k$, whereas in the three-pylon configuration it is restricted to $m = \pm 3k$. In most cases, the dominant reflected contributions are associated with the highest cut-on azimuthal orders allowed by the frequency. By contrast, the reflected level of the incident axisymmetric mode remains comparatively weak.

At $f = 800$ Hz, the reflected levels are markedly higher for the three-pylon configuration than for the two-pylon one. A likely explanation is that the scattered modes with $m = \pm 3$ lie closer to cut-off than the modes with $m = \pm 2$, which tends to enhance their sensitivity to the impedance change induced by the pylon row.

The transmitted field exhibits a different behavior. In all cases, the axisymmetric mode remains the most energetic transmitted component, as expected from the axisymmetric nature of the incident plane wave. For $f \geq 800$ Hz, however, non-axisymmetric transmitted contributions also appear at orders $m = \pm 2k$ and $m = \pm 3k$ for the two- and three-pylon ducts, respectively. Unlike the reflected field, the transmitted levels are not systematically maximal near cut-off, and their variations with frequency are clearly non-monotonic. At the highest frequency, $f = 3200$ Hz, the transmitted levels of the cut-on scattered modes differ by only a few decibels over a broad range of azimuthal orders, which reflects a much broader redistribution of acoustic energy.

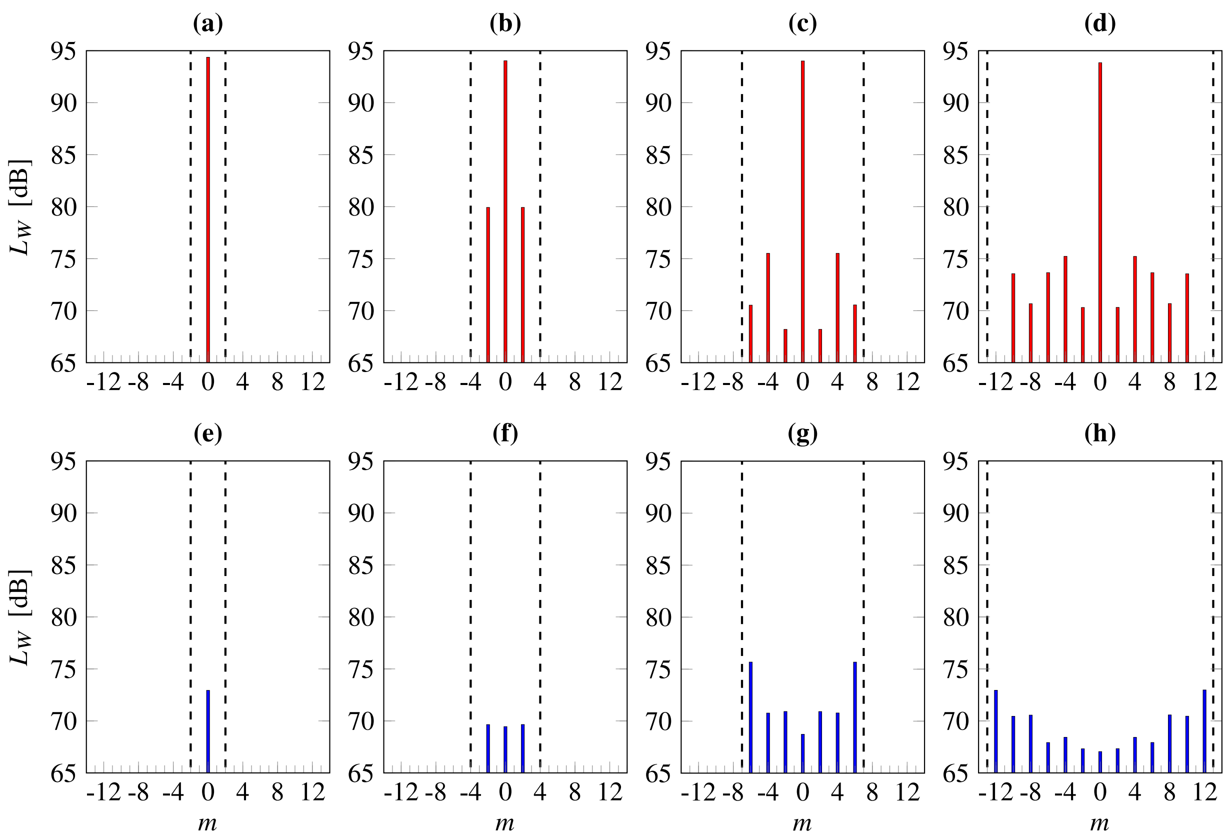

Fig. 6 Sound power levels obtained for incident plane wave for the —— transmitted and —— reflected azimuthal modes for (a,e) $f = 400$ Hz, (b,f) 800 Hz, (c,g) 1600 Hz, and (d,h) 3200 Hz for the duct with two pylons; - - - - - first cut-off azimuthal mode.

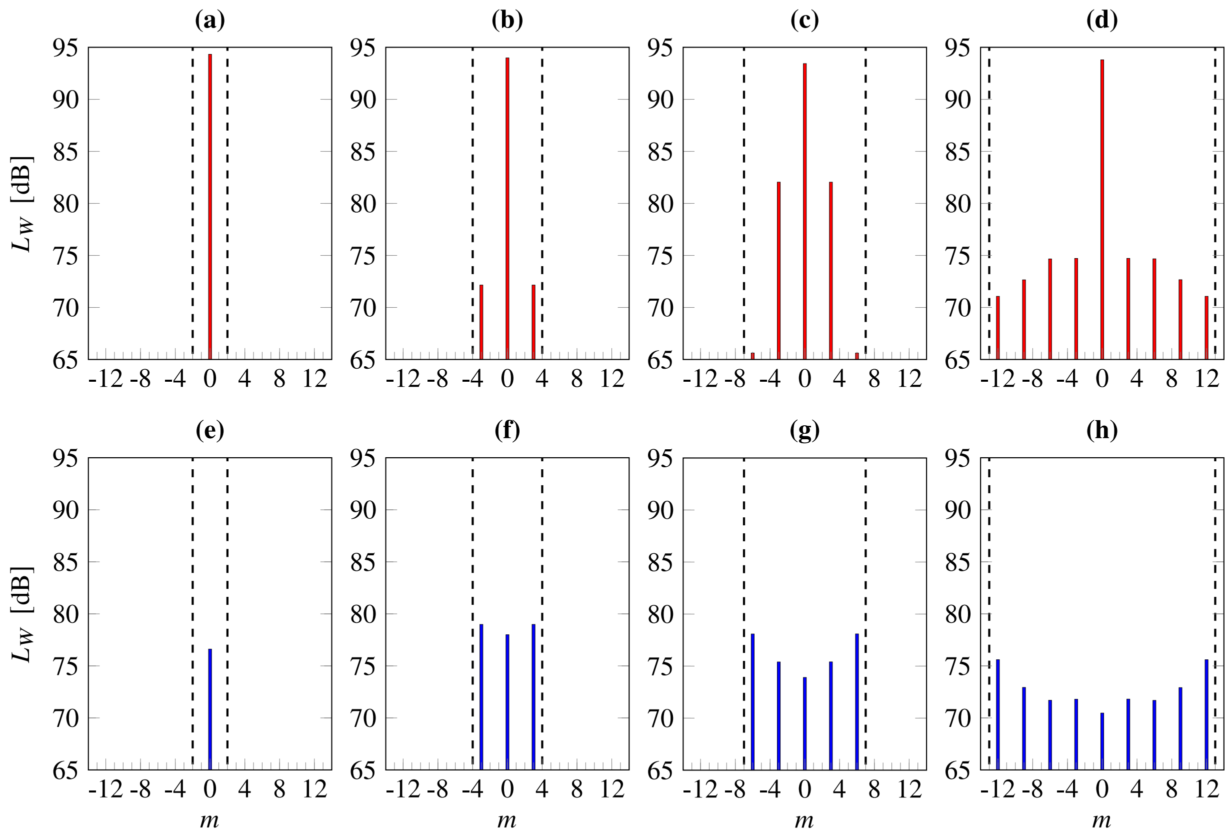

Fig. 7 Same as Figure 6 but for the duct with three pylons.

D. Higher-order azimuthal modes propagation

The propagation of incident higher-order azimuthal modes with order $m = 1$–8 is now examined using the modal maps shown in Figures 8 and 9, which display the sound power levels of the transmitted and reflected azimuthal modes as functions of both the incident azimuthal order and the scattered azimuthal order. The results show that the scattering of incident spinning modes remains primarily governed by the azimuthal periodicity of the pylon row. Indeed, the scattered components satisfy a selection rule of the form $m = m_{\text{inc}} \pm kN_p$, where m_{inc} is the azimuthal order of the incident mode, N_p is the number of pylons, and k is an integer. Thus, for the two-pylon duct, the scattered energy is redistributed among modes separated by multiples of 2, whereas for the three-pylon duct it is redistributed among modes separated by multiples of 3. This generalizes the observations made for incident plane waves and confirms that the pylon row acts as an azimuthally periodic scattering element. At low frequency, only a limited number of scattered components are cut on, and the transmitted field therefore remains concentrated around the incident mode. As the frequency increases, more azimuthal and radial modes become propagative, and the scattering broadens significantly. A particularly noteworthy result is that, for some incident spinning modes and frequencies, the dominant transmitted mode has an azimuthal order of opposite sign to that of the incident mode. In other words, the pylon row can transfer most of the transmitted acoustic energy to a mode rotating in the opposite azimuthal direction. This suggests that, beyond simple modal redistribution, the bifurcation row may substantially alter the apparent spinning character of the acoustic field downstream of the pylons. This phenomenon is clearly visible for $f = 800$ Hz and $m_{inci} = 2$ in Figures 8(b) and 9(b).

To shed further light on the mode-reversal phenomenon, the pressure fields obtained on the outer surfaces of the duct for $f = 800$ Hz and $m_{inc} = 1$, 2, and 3 are shown in Figures 10(a-f). In all cases, strong scattering is observed. For $m_{inci} = 2$ and for the duct with two pylons in Figure 10(b), the reversal of the spinning mode through its propagation across the pylons is clearly visible. For $m_{inci} = 3$ and for both ducts in Figures 10(c,f), the levels are particularly high upstream of the pylons, and low downstream, indicating that most of the energy of the incident mode is reflected by the pylons. This can be explained by the fact that the cut-on frequency of the mode $m = 3$ is very close to $f = 800$ Hz, its propagating angle being very close to 90° relative to the duct axis.

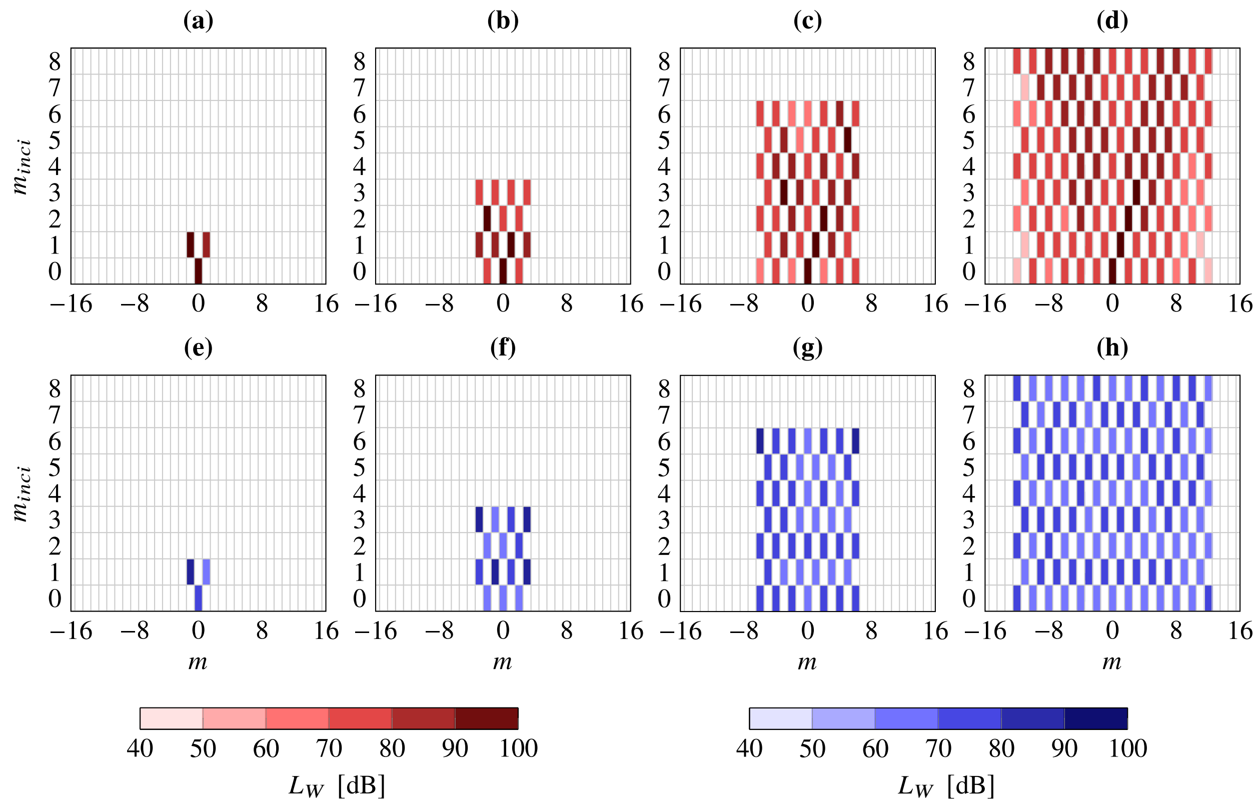

Fig. 8 Sound power levels of the (a-d) transmitted and (e-h) reflected modes as functions of the incident azimuthal order m_{inc} and scattered azimuthal order m, for (a,e) f = 400 Hz, (b,f) f = 800 Hz, (c,g) f = 1600 Hz, and (d,h) f = 3200 Hz, for the duct with two pylons.

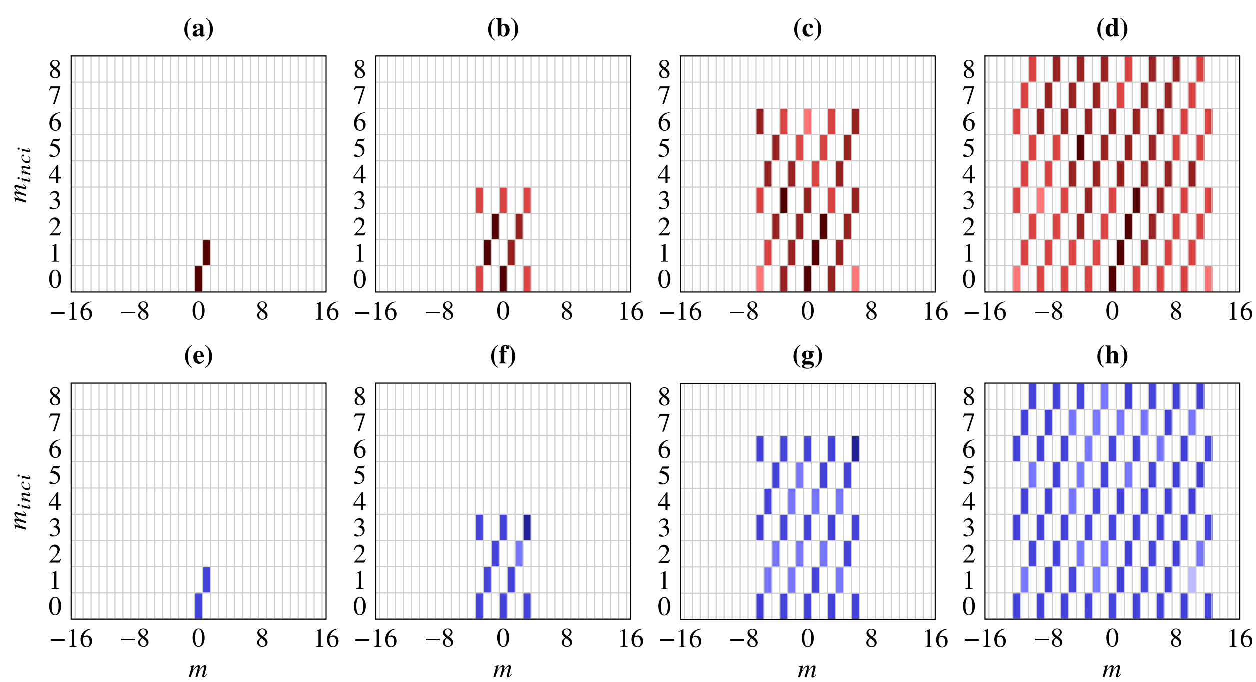

Fig. 9 Same as Figure 8 but for the duct with three pylons.

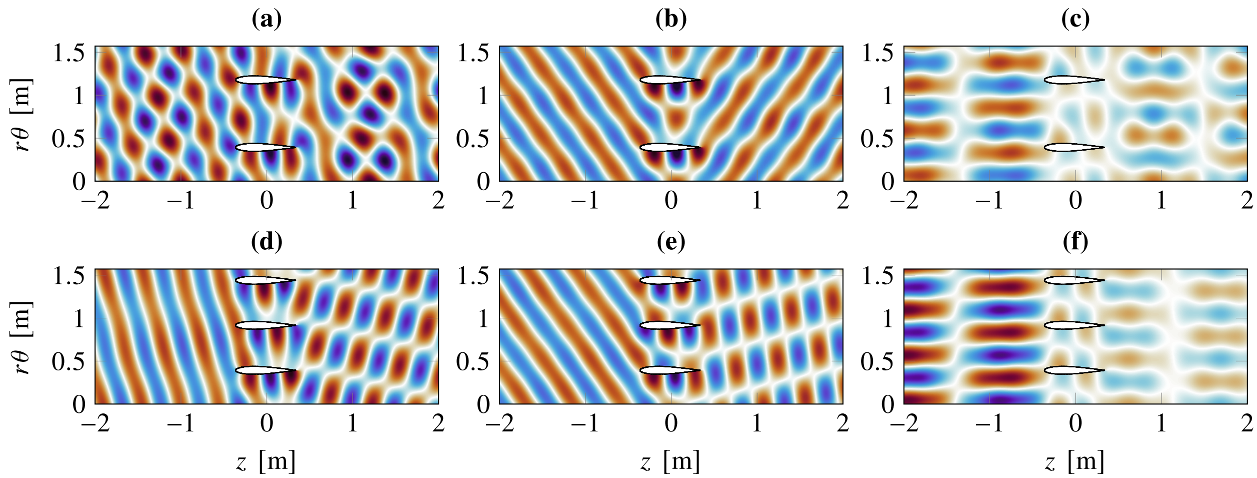

Fig. 10 Pressure fields obtained for the annular ducts with (first row) two pylons and (second row) three pylons, for (first column) m_{inci} = 1, (second column) m_{inci} = 2, and (third column) m_{inci} = 3, for f = 800 Hz. The color scale is the same as in Figure 4.

E. Effect of a non-uniform mean flow

The cut-on azimuthal and radial modes for M = 0, 0.2, and 0.4 are shown in Figure 11. The four frequencies investigated in the simulations are also indicated. For f = 400, 800, and 1600 Hz, only modes with the lowest radial order are cut on, whereas at f = 3200 Hz modes with higher radial orders also propagate. Increasing the Mach number only slightly modifies the cut-on limits, but this can nevertheless affect the scattered modal content. In particular, for M = 0.4, the modes $m = \pm 14$ become cut on, whereas they remain cut off for the lower-Mach-number cases.

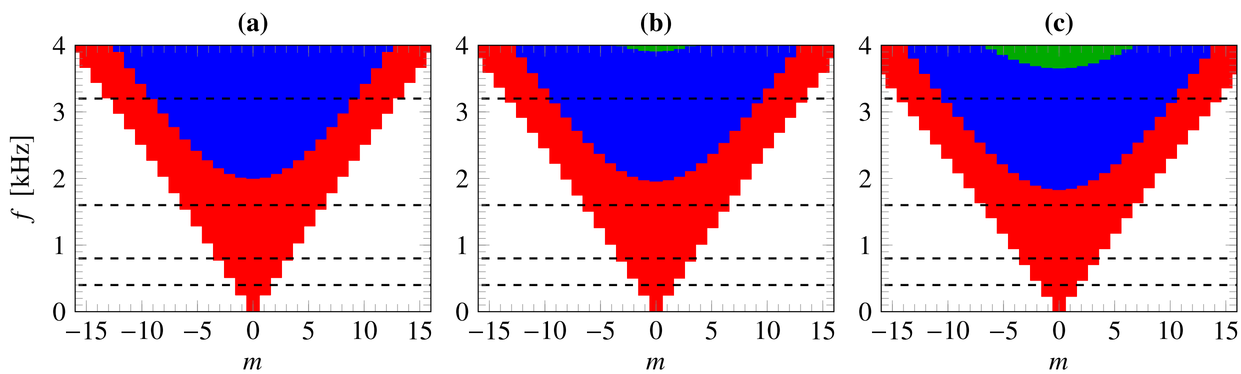

Fig. 11 Cut-on frequencies of the annular duct modes with n = 0, n = 1, and n = 2, for (a) M = 0, (b) M = 0.2, and (c) M = 0.4; - - - - - frequencies considered for the simulations.

To illustrate the effect of mean flow on the acoustic propagation, pressure fields obtained without flow and with mean flows at Mach numbers 0.2 and 0.4 are shown for the two- and three-pylon configurations in Figures 12(a,c,e) and 12(b,d,f). For both geometries, the wavelength of the transmitted waves downstream of the pylons increases with Mach number, as expected. In addition, the pressure fields upstream of the pylon row become more complex as the Mach number increases, with more pronounced azimuthal variations.

The sound power levels of the transmitted and reflected azimuthal modes obtained for the different Mach numbers are shown in Figures 13 and 14 for the ducts with two and three pylons, respectively. In both configurations, the modal content remains primarily governed by the azimuthal periodicity of the pylon row, with dominant contributions at $m = \pm 2k$ for the two-pylon duct and $m = \pm 3k$ for the three-pylon duct. For the transmitted field, shown in Figures 13(a-c) and 14(a-c), the axisymmetric mode remains dominant at all Mach numbers, while non-axisymmetric contributions appear for $f \geq 800$ Hz. The influence of the mean flow on the transmitted levels is weak at f = 400 Hz, but becomes more pronounced as the frequency increases. At f = 1600 Hz, noticeable variations in the relative amplitudes of the scattered modes are observed, although the overall modal distribution remains similar. For the reflected field, shown in Figures 13(d-f) and 14(d-f), the effect of Mach number is slightly stronger. At $f = 400$ Hz, only a few modes contribute and their levels are only weakly affected by the flow. By contrast, at higher frequencies, significant variations are observed, with both amplification and attenuation of specific modes depending on the Mach number. Overall, the influence of the mean flow is non-monotonic with respect to the number of pylons, frequency, and Mach number.

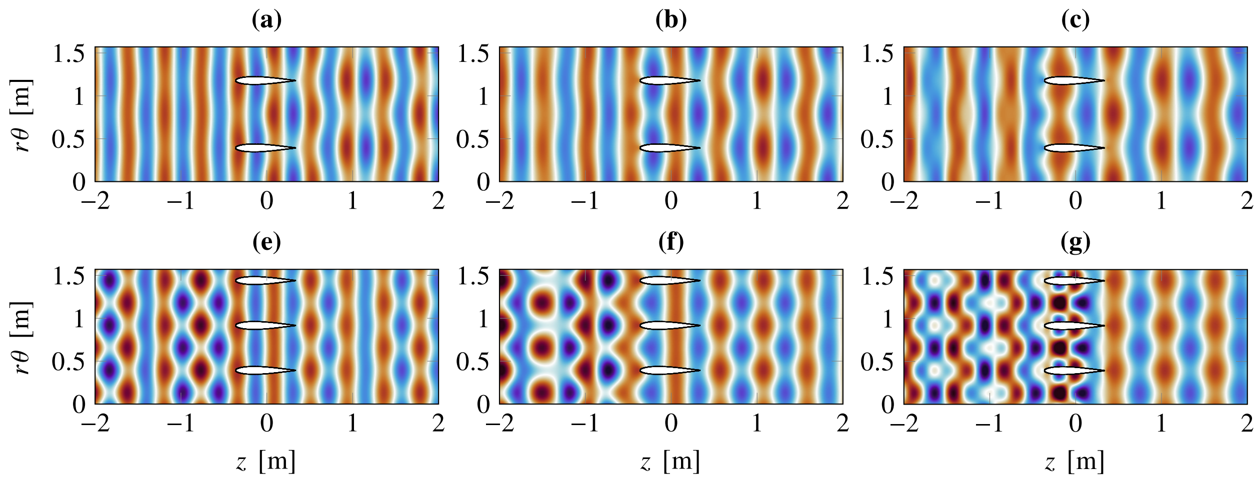

Fig. 12 Pressure fields obtained for incident plane wave for the annular ducts with (first row) two pylons and (second row) three pylons, for (first column) M = 0, (second column) M = 0.2, and (third column) M = 0.4, for f = 800 Hz. The color scale is the same as in Figure 4.

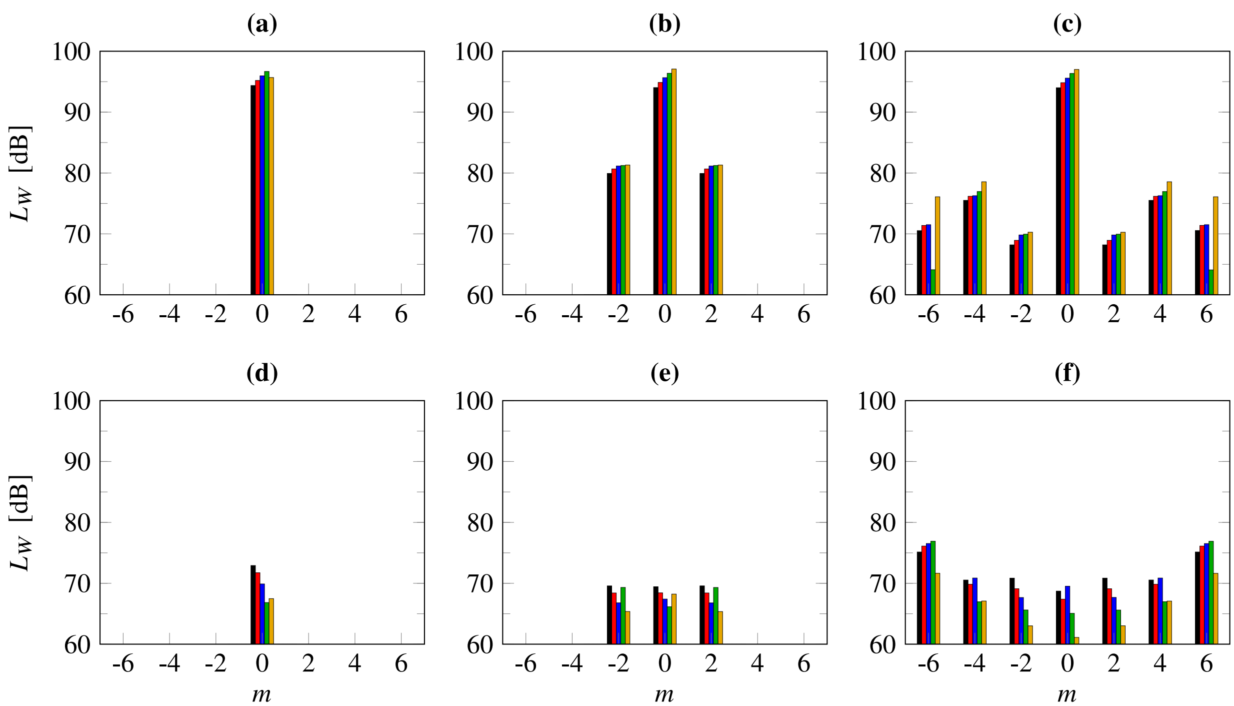

Fig. 13 Sound power levels of the (a-c) transmitted and (d-f) reflected azimuthal modes (a,d) f = 400 Hz, (b,e) f = 800 Hz, and (c,f) f = 1600 Hz, for M = 0, M = 0.1, M = 0.2, M = 0.3, and M = 0.4, for the duct with two pylons.

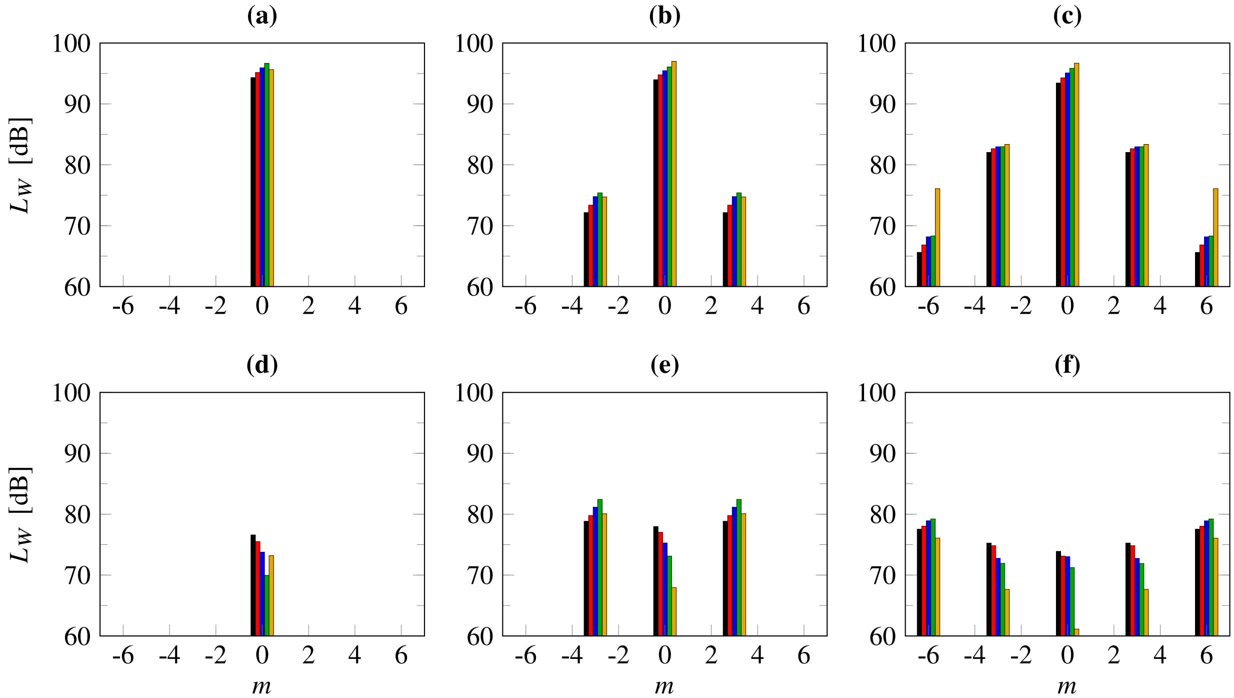

Fig. 14 Same as Figure 13 but for the duct with three pylons.

IV. Conclusions

The scattering of acoustic modes by pylon rows in annular ducts has been investigated numerically for configurations with two and three pylons, in quiescent conditions and with a non-uniform mean flow up to M = 0.4. A good overall agreement was obtained between the numerical and experimental azimuthal spectra, which supports the validity of the numerical framework. For incident plane waves, the scattered azimuthal content is governed mainly by the number of pylons, in agreement with the Tyler-Sofrin rule. The strongest reflected modes are found close to cut-off, whereas the transmitted field remains dominated by the axisymmetric mode while still showing redistribution toward non-axisymmetric components. As the frequency increases, the scattering becomes broader because more modes become cut on. For incident higher-order azimuthal modes, the same selection rule remains valid. In some cases, the dominant transmitted mode has an azimuthal order of opposite sign to that of the incident mode, indicating a reversal of the dominant spinning direction. Mean flow does not modify the modal selection rule, but it significantly affects the scattered amplitudes in a non-monotonic way.

Future work will focus on the optimization of microphone arrays for modal decomposition in bifurcated annular ducts, building on the experimental framework of Behn et al. [18]. It will also address the validation of analytical models, in particular the mode-matching approach described by Girier & Leclère [21], by direct comparison with the high-fidelity simulations.

Acknowledgments

This research has been performed in the frame of the project COMPANION (COMmon Platform and Advanced iNstrumentration readIness for ultra efficient propulsiON) - Grant Agreement No. 101140627. The project is supported by the Clean Aviation Joint Undertaking and its members. Funded by the European Union. Views and opinions expressed are however those of the author(s) only and do not necessarily reflect those of the European Union or Clean Aviation Joint Undertaking. Neither the European Union nor Clean Aviation JU can be held responsible for them.

References

[1] Moreau, S., "Turbomachinery noise predictions: present and future," *Acoustics*, Vol. 1, No. 1, 2019. https://doi.org/10.3390/acoustics1010008.

[2] Lewis, D., de Laborderie, J., Sanjosé, M., Moreau, S., Jacob, M. C., and Masson, V., "Parametric study on state-of-the-art analytical models for fan broadband interaction noise predictions," *J. Sound Vib.*, Vol. 514, 2021, p. 116423. https://doi.org/10.1016/j.jsv.2021.116423.

[3] Salze, E., Pereira, A. A., Brandstetter, C., Clair, V., Gea-Aguilera, F., Lamidel, D., Marjono, J., Buszyk, M., Polacsek, C., Maier, R., Stanica, C., Dragan, V., Stanescu, T., and Bauer, M., "Noise reduction of aero-engines using innovative stators with leading edge features," *AIAA Paper 2024-3159*, 2024. https://doi.org/10.2514/6.2024-3159.

[4] Al-Am, J., Giauque, A., Clair, V., Boudet, J., and Gea-Aguilera, F., "Direct-noise of an ultrahigh-bypass-ratio turbofan: periodic-sector vs full-annulus large-eddy simulations," *AIAA J.*, Vol. 62, No. 8, 2024, pp. 2831–2845. https://doi.org/10.2514/1.J063596.

[5] Tyler, J. M., and Sofrin, T. G., "Axial flow compressor noise studies," *SAE Tech. Pap.*, 1962. https://doi.org/10.4271/620532.

[6] Panek, L., Schönwald, N., Richter, C., and Thiele, F., "Simulation of the rearward propagation of fan noise through a long cowl aero-engine," *AIAA Paper 2008-2820*, 2008. https://doi.org/10.2514/6.2008-2820.

[7] Chen, X., Huang, X., and Zhang, X., "Sound radiation from a bypass duct with bifurcations," *AIAA J.*, Vol. 47, No. 2, 2009, pp. 429–436. https://doi.org/10.2514/1.39710.

[8] Redonnet, S., and Druon, Y., "Computational aeroacoustics of aft fan noises characterizing a realistic coaxial engine," *AIAA J.*, Vol. 50, No. 5, 2012, pp. 1029–1046. https://doi.org/10.2514/1.J050730.

[9] Nark, D., Farassat, F., Pope, D., and Vatsa, V., "Effects of bifurcations on aft-fan engine nacelle noise," *AIAA Paper 2004-2988*, 2004. https://doi.org/10.2514/6.2004-2988.

[10] Schönwald, N., Panek, L., Richter, C., and Thiele, F., "Mode propagation in bifurcated bypass ducts: application oriented simulation approach," *AIAA Paper 2010-3895*, 2010. https://doi.org/10.2514/6.2010-3895.

[11] Holewa, A., Weckmüller, C., and Guérin, S., "Impact of bypass duct bifurcations on fan noise," *J. Propuls. Power*, Vol. 30, No. 1, 2014, pp. 143–152. https://doi.org/10.2514/1.B34957.

[12] Bonneau, V., Polacsek, C., Barrier, R., Lewy, S., Roux, J.-M., and Gervais, Y., "Tonal noise prediction of a turbofan with heterogeneous stator and bifurcations," *AIAA J.*, Vol. 53, No. 11, 2015, pp. 3354–3369. https://doi.org/10.2514/1.J053970.

[13] Sugimoto, R., Astley, R. J., Mercato, L. D., Holland, K., and Jurdic, V., "Prediction methods for propagation in bypass ducts and comparison with measured data," *AIAA Paper 2005-3059*, 2005. https://doi.org/10.2514/6.2005-3059.

[14] Sugimoto, R., Astley, J., Gabard, G., and Tsuchiya, N., "Three-dimensional effects of geometries and acoustic treatments on bypass-duct noise," *AIAA Paper 2007-3549*, 2007. https://doi.org/10.2514/6.2007-3549.

[15] McAleer, C., Astley, R. J., Holland, K., Sugimoto, R., and Kempton, A., "Fan noise propagation within curved bypass ducts with 3D features," *AIAA Paper 2008-2878*, 2008. https://doi.org/10.2514/6.2008-2878.

[16] Panek, L., Schönwald, N., Richter, C., and Thiele, F., "Mode propagation in bifurcated bypass ducts: elementary mechanisms," *AIAA Paper 2010-3894*, 2010. https://doi.org/10.2514/6.2010-3894.

[17] Schönwald, N., Lück, H., Panek, L., Thiele, F., and Richter, C., "Numerical investigation of mean flow and liner effects on the mode propagation in a bifurcated bypass duct," *AIAA Paper 2011-2726*, 2011. https://doi.org/10.2514/6.2011-2726.

[18] Behn, M., Tapken, U., Vincent, H., Pereira, A., and Jacob, M. C., "Experimental study on sound propagation through a duct section with large pylons," *AIAA Paper*, 2026. Submitted.

[19] Behn, M., Klähn, L., and Tapken, U., "Comprehensive experimental investigation of mode transmission through stator vane rows: Results and calibration of an analytical prediction model," *AIAA Paper 2017-3218*, 2017. https://doi.org/10.2514/6.2017-3218.

[20] Knobloch, K., Grizewski, L., Kohlenberg, H.-F., Behn, M., and Genssler, J., "Framework for modal based assessment of liner structures," *AIAA Paper 2024-3298*, 2024. https://doi.org/10.2514/6.2024-3298.

[21] Girier, L., Leclère, Q., Behn, M., and Tapken, U., "On a mode-matching technique for acoustic scattering by an annular row of airfoil-shaped pylons," *AIAA Paper*, 2026. Submitted.

[22] Rienstra, S. W., "Fundamentals of duct acoustics," *Von Karman Institute Lecture Notes*, 2015.

[23] Möhring, W., "A well posed acoustic analogy based on a moving acoustic medium," *Aeroacoustic Workshop SWING*, 1999.

[24] Geuzaine, C., and Remacle, J.-F., "Gmsh: A 3-D finite element mesh generator with built-in pre- and post-processing facilities," *Int. J. Numer. Methods Eng.*, Vol. 79, No. 11, 2009. https://doi.org/10.1002/nme.2579.